Paleomagnetic stratigraphy across the Eocene-Oligocene Boundary at Monte Cagnero (Piobbico, Northeastern Apennines, Italy): Correlations to the GSSP at Massignano (Ancona, Italy)

Ethan G. Hyland
Senior Integrative Exercise
March 10, 2008

Submitted in partial fulfillment of the requirements for a Bachelor of Arts degree from Carleton College, Northfield, Minnesota.

Table of Contents

Paleomagnetic stratigraphy across the Eocene-Oligocene Boundary at Monte Cagnero (Piobbico, Northeastern Apennines, Italy): Correlations to the GSSP at Massignano (Ancona, Italy)

Ethan G. Hyland
Senior Integrative Exercise
March 10, 2008

Advisors:
Cameron Davidson, Carleton College
Alessandro Montanari, Osservatorio Geologico di Coldigioco
David A. Evans, Yale University

Abstract

A forty meter section of Scaglia Cinerea was sampled for paleomagnetic stratigraphy across the Eocene-Oligocene boundary at Monte Cagnero, Piobbico, Italy. Ninety-two oriented cores were obtained and progressive alternating field and thermal demagnetization isolated distinct ChRM components in most samples. Stable endpoint components with coercivities from 15-40 mT and unblocking temperatures from 300-340°C or 550-580°C indicated carriers of pyrrhotite and magnetite (primary), and a stratigraphic plot of these components defines distinct normal and reversed magnetozones. These magnetozones create a polarity sequence which directly correlates to chrons C13r to C12n of the geomagnetic polarity timescale, including two short cryptochrons C13r-1 and C12r-8. The magnetostratigraphy is also consistent with the Massignano GSSP. Virtual geomagnetic pole plots (λ= 71°, ϕ=209°) indicate correlation to the synthetic apparent polar wander path for the Adrian Promontory/African Plate during the Eocene and Oligocene. Anisotropy of magnetic susceptibility data indicates some inclination shallowing in Scaglia sediments. This study provides preliminary support for the viability of Monte Cagnero as a site for the relocation of the Eocene-Oligocene global stratotype section and point.

Keywords: magnetostratigraphy; paleomagnetism; Eocene; Oligocene; Scaglia Cinerea; Massignano GSSP, Italy; apparent polar wander.

Introduction

The Eocene-Oligocene transition records a period of major geologic change including profound evolutions in worldwide climate, oceanography and geography (Prothero, 1994). The transition occurred over a period of a few hundred thousand years during which the planet's climate system deteriorated from a "greenhouse" climate, or warm, humid period, to an "icehouse" climate, characterized by accelerated global cooling and formation of significant polar ice sheets (e.g. Zachos et al., 2001; van Mourik et al., 2007). This climatic transition is responsible for major changes in both marine and terrestrial biodiversity, and is considered one of the most extreme global changes of the past 50+ million years (Prothero, 1994).

The Eocene-Oligocene boundary is currently defined as the extinction/last occurrence (LO) of the planktonic foraminifera *Hantkenina* and *Cribrohantkenina* (Eocene genera of the *Hantkeninidae*), occurring at approximately 33.7 ± 0.01 Ma (Brown, *unpublished;* Jovane et al., 2006). The Global Stratotype Section and Point (GSSP) is located 19m above the base of the section at the Massignano quarry outside of Ancona, Italy (Premoli-Silva and Jenkins, 1993; Fig. 1). Recent studies suggest the possibility that the Eocene-Oligocene boundary may be better defined as a longer transitional period involving bolide impacts (c.f. Bodiselitsch et al., 2004; Montanari and Koeberl, 2000), comet showers (c.f. Farley et al., 1998) and major global isotope excursions of $\delta^{18}O$ and $\delta^{13}C$ (c.f. Salamy and Zachos, 1999; Zachos et al., 2001). These global isotope excursions, including the Oi1 event, a $\delta^{18}O$ shift of ~1.2‰ occurring between 33.48 and 33.6 Ma that suggests massive glaciations (Zachos et al., 2001), are indicators of extreme climate change, which might provide a more legitimate and globally recognizable epoch boundary (Montanari, 1988; Bohaty et al., 2007; van Mourik et al., 2007).

Complete sequences of the rock record for this time period are exceedingly rare. However, in the Umbria-Marche basin of the Northeastern Apennine mountains, the boundary is well-preserved within the Scaglia Cinerea Formation in a number of locations (Fig. 1). Further, integrated stratigraphic data (including lithostratigraphy, biostratigraphy, magnetostratigraphy and cyclostratigraphy) are available for exposures such as the Contessa Valley (Lowrie et al., 1982), Monte Cagnero (Coccioni et al., *in press*), and the Massignano quarry GSSP (Alvarez and Montanari, 1988, Napoleone, 1988, Coccioni et al., 1988, Odin et al., 1988a,b, Bice and Montanari, 1988, Premoli Silva and Jenkins, 1993). The Scaglia Cinerea Formation falls near the top of a complete and primarily undisturbed pelagic carbonate succession, and is characterized by fossiliferous marly limestone and calcareous marl. In addition, it contains a handful of radiometrically dated volcanic ash and biotite-rich volcaniclastic layers (Montanari et al., 1988), which provide independent age constraints for detailed stratigraphic studies.

The Massignano section continues only 8m beyond the recognized E/O boundary, and therefore does not contain the entirety of the Oi1 isotope excursion which could provide a more correlatable and appropriate epoch boundary. The section at Monte Cagnero, unlike Massignano (~27m), is continuous for a few hundred meters and contains the entirety of the upper Eocene and the Oligocene, including the full extent of the isotope shift. The base of this section appears to correlate to the base of the Massignano quarry (Coccioni et al., *in press*), but no further research had been done, aside from basic lithostratographic analysis, biostratigraphy, and marking (Lowrie et al., 1982; Parisi et al., 1988), in the section containing the Eocene-Oligocene shift. However, Coccioni et al. (*in press*)

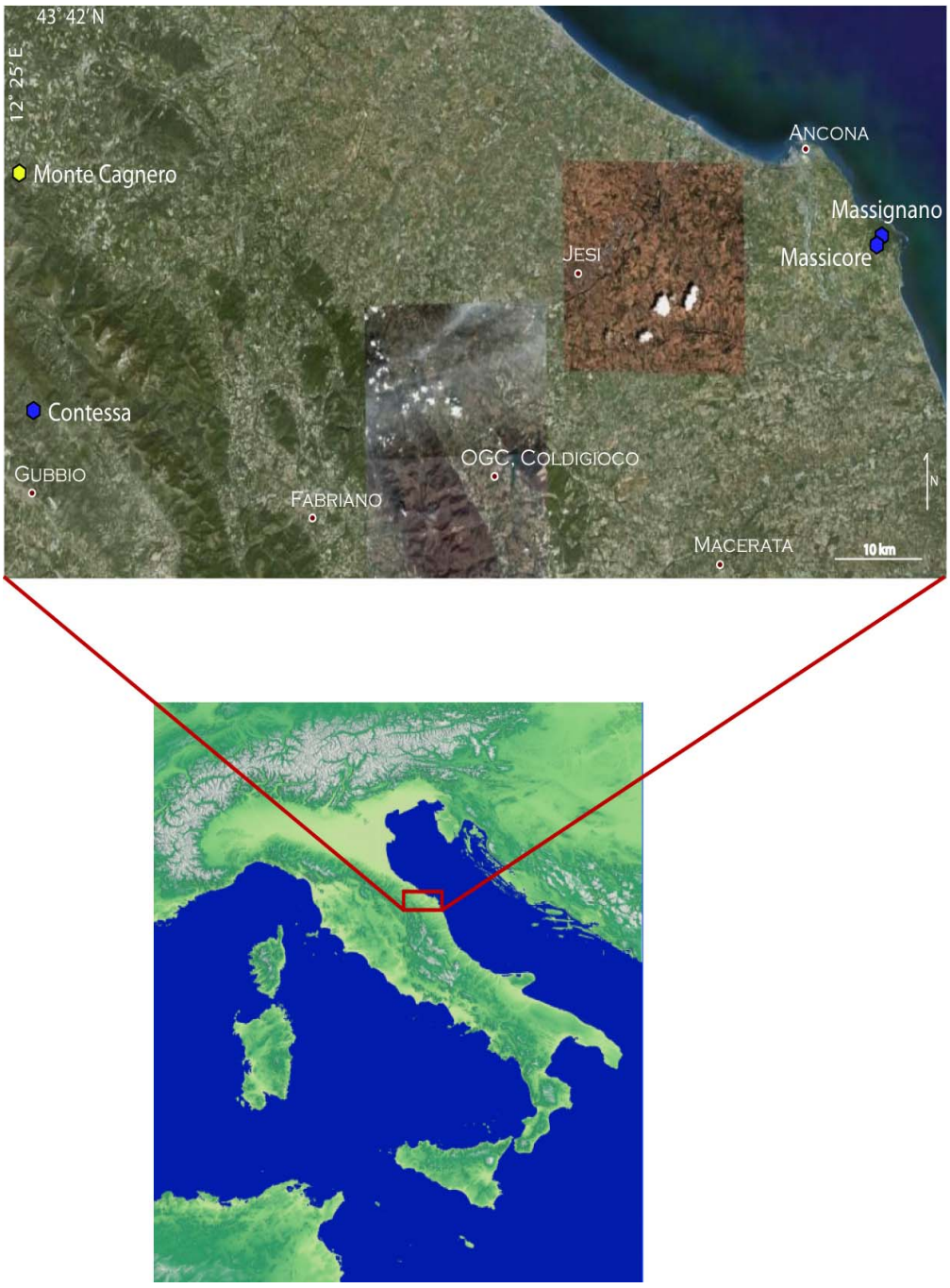

Figure 1. Location map of the Marche region of Italy, with important Scaglia Cineria Formation sections marked in blue, and this study in yellow. Landsat image from GoogleEarthPlus.

have completed litho-, bio-, chemo-, and magnetostratigraphy of the section from meters 145 to 225.

Magnetostratigraphic studies conducted successfully in various marine sedimentary rocks, including the pelagic limestone sequences of central Italy, allow definitive correlations to the geomagnetic polarity time scale (GPTS) and paleontological stage boundaries for the Eocene/Oligocene boundary (Contessa: Lowrie et al., 1982, and Nocchi et al., 1986; Massignano/MassiCore: Bice and Montanari, 1988, Lowrie and Lanci, 1994, and Lanci et al., 1996).

A full paleomagnetic study performed for this site provides accurate dating of the section based on the geomagnetic polarity time scale (Cande and Kent, 1992, 1995), allows correlation of this section to well-known exposures, and establishes the groundwork for future work on stable isotopes, mineralogy, and biostratigraphy in the region to determine whether the Monte Cagnero site is a viable option for relocating the Eocene-Oligocene boundary GSSP.

Geologic Setting and Methods

Forty meters of the Scaglia Cinerea Formation at Monte Cagnero (Fig. 2) was logged for rock type and color predicated on previously established section markers and stratigraphic succession. Coccioni et al. (*in press*) indicate an approximate stratigraphic equivalency between meter level 100 at Monte Cagnero and meter level 0 at Massignano based on preliminary lithologic and contextual comparison.

The section (including from a fault/slump at meter level 108 to the base of the section studied in Coccioni et al., *in press*, at meter 145), is mostly green-brown or pink marly limestones/calcareous marls. The section contains two significant biotite-rich volcaniclastic layers at meters 142.8 (dated by Montanari et al., 1988) and 144.8,

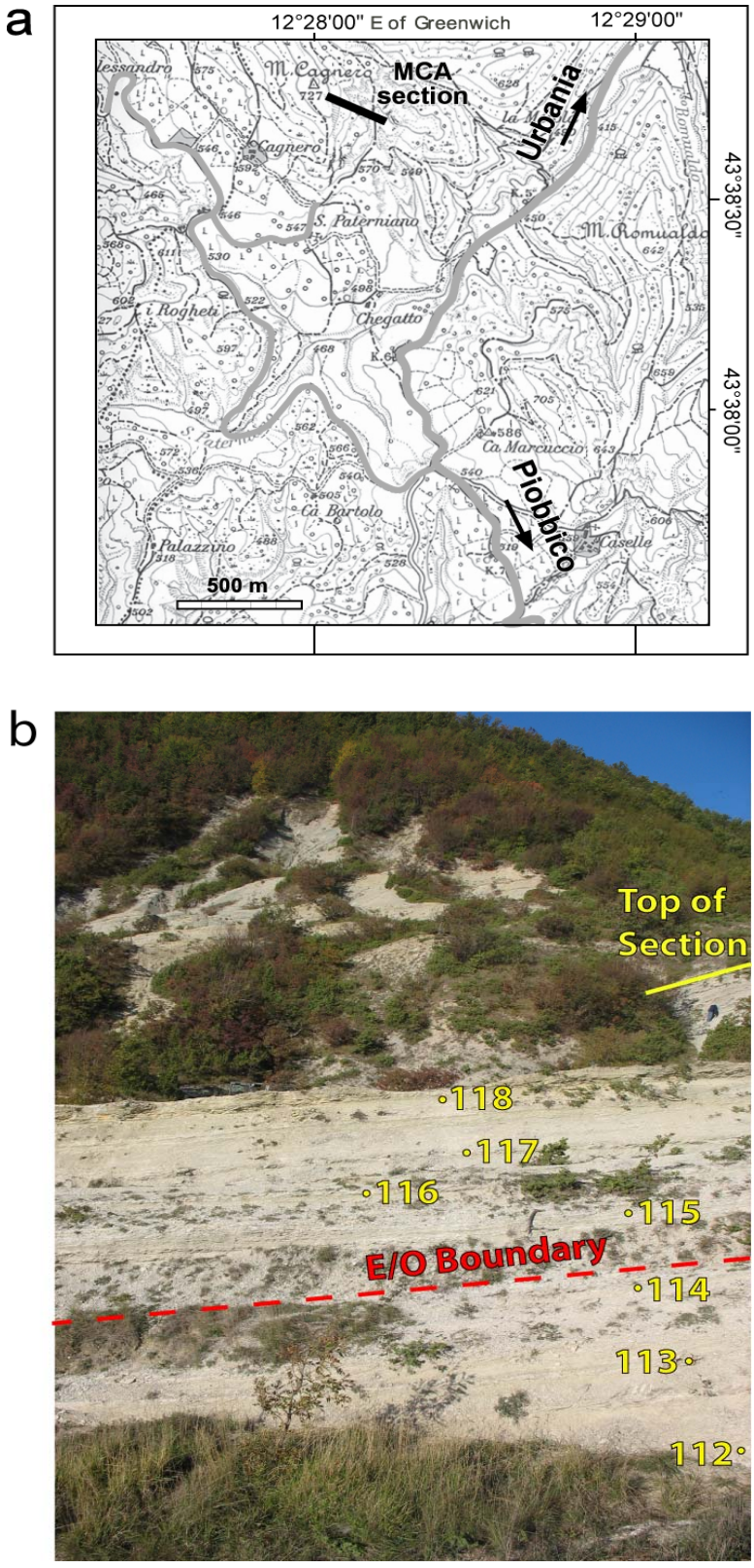

Figure 2. (A) Location of Monte Cagnero section (modified from Coccioni et al., *in press*). (B) Outcrop photo with meter levels and important features shown.

which provide tie-points for accurate chronostratigraphy. The section also contains the last occurence (LO) for the genera *Hantkeninidae* at approximately meter level 114.5 (Montanari et al., 2007; Tori and Monechi, 2007), serving as a marker for the currently recognized E/O boundary.

Samples for the analysis of calcium carbonate content and magnetic susceptibility were taken every 0.05m for meters 133-150 (meter system from Coccioni et al., *in press*). The calcium carbonate content and magnetic susceptibility samples were powdered in a brass mortar and analyzed with a Dietrich-Fruling water calcimeter (±2% error), in a 10% HCl solution; and a Bartington MS2/MS2B dual frequency sensor on low frequency (0.465kHz) and sensitivity (x0.1), calibrated for thermal drift.

Oriented paleomagnetism hand-samples were taken at 0.5m intervals throughout this segment of the Monte Cagnero section (meters 108-145). The paleomagnetic samples were then cut down and oriented in concrete with respect to the horizontal bedding plane and cored (while maintaining orientation) using a 2.5 cm-diameter drill press at the Osservatorio Geologico di Coldigioco (OGC) in Coldigioco, Italy.

Paleomagnetic measurements were carried out using an automatic cryogenic DC-SQuID magnetometer in a magnetically shielded room at the Yale Department of Geology and Geophysics (New Haven, CT), under the direction of David Evans. The samples (n= 92) were pre-cleaned with liquid nitrogen in a zero field to preferentially reduce multidomain carriers and then treated with low alternating frequency (AF; 0-10 mT, 2 mT increments) and low thermal (TT; 75˚C-200˚C, 25˚C increments) demagnetization processes. Samples were then split into two populations, with at least one core from every stratigraphic level in each; population A-C (n= 51) was

further treated with high AF (15-70 mT at 5 mT increments), while population B (n= 41) was treated with high thermal (250-580˚C at increments of between 10˚C and 50˚C depending on proximity to known unblocking temperatures) in a controlled N_2 environment to prevent the accidental oxidation of weakly magnetized sediments (most samples had magnetizations of $<10^{-6}$ G). The isolated characteristic remnant magnetization (ChRM) data from these samples were then determined and analyzed using PaleoMag v 3.1b1, where bedding, tilt, and misoriented sample corrections were made and statistical models were applied (least squares models, Fisher statistics, Bingham test, etc., after Fisher, 1953; Zijderveld, 1967; Kirschvink, 1980).

After ChRM analysis, samples were chosen to be measured for anisotropy. Alternate, untreated samples were selected based on polarity group and on the presence of alteration minerals (goethite and pyrrhotite), and then evaluated using an AGICO KLY-4S anisotropy of magnetic susceptibility (AMS) system to determine overall rock anisotropy with regard to magnetization directions.

Results and Paleomagnetism

Calcium carbonate content (%$CaCO_3$) is relatively constant throughout the outcrop (Fig. 3), generally remaining between 60% and 70%, with a slight upward trend corresponding to the up-section lithologic increase in competence of the limestone. Magnetic susceptibility displays, as anticipated, the inverse relationship, decreasing in intensity as the section becomes predominantly limestone. These values are on average around 35 in the marly section (meters 133-142), with some values reaching as high as 90, while higher in the section (meters 142-150), values appear much lower, around 10-15. The calcium carbonate content and

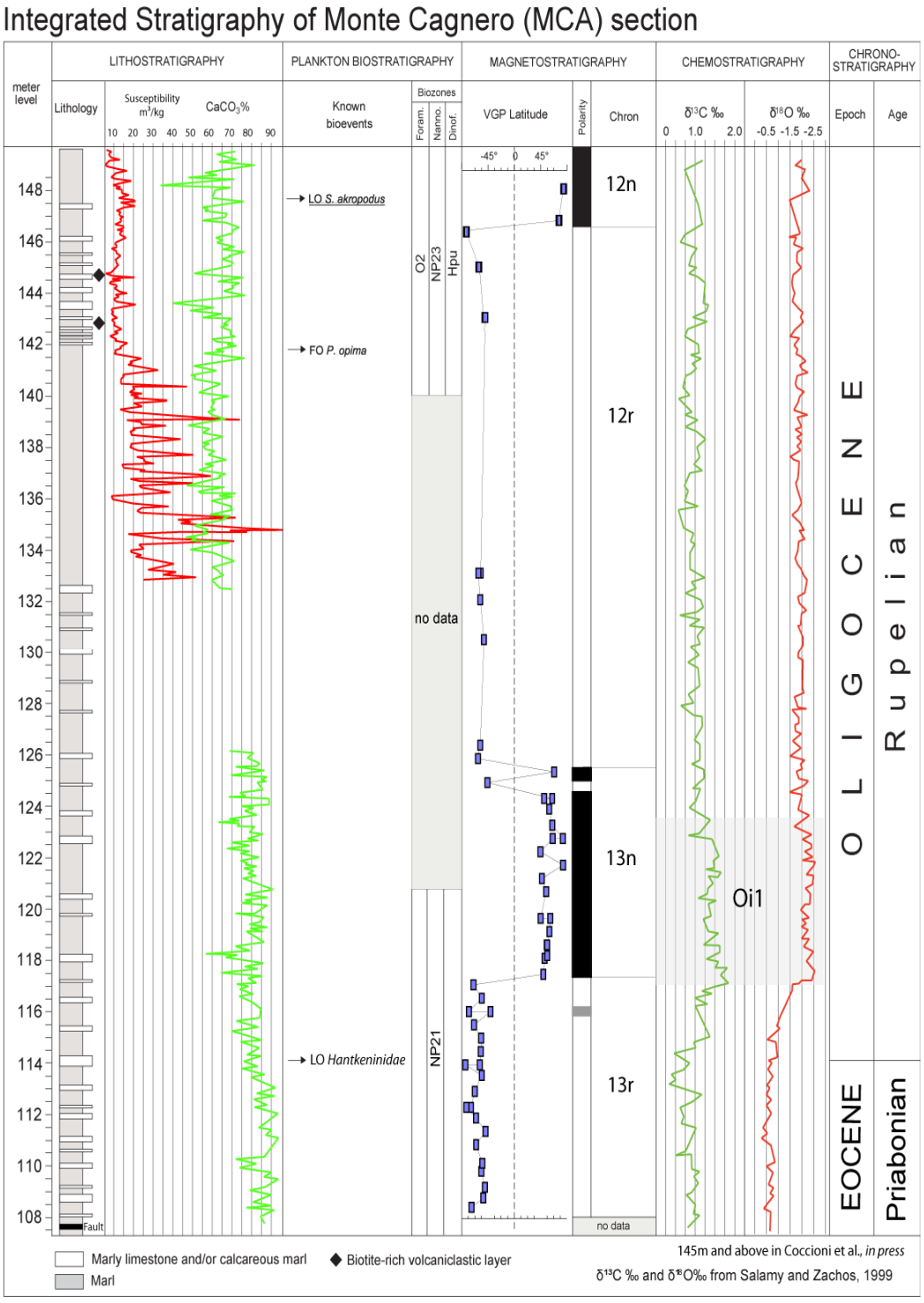

Figure 3. Integrated stratigraphy of Monte Cagnero, showing lithostratigraphy, magnetostratigraphy, and available bio- and chemostratigraphy (Coccioni et al., *in press*; Salamy and Zachos, 1999).

magnetic susceptibility data were not analyzed in detail, and are therefore presented merely as further information in the preliminary exploration of this outcrop, though they could serve as a starting point for the cyclostratigraphic or chemostratigraphic analysis of the section.

The primary objective of paleomagnetic reversal stratigraphy is to discern the timing of past geomagnetic field configurations. This is based on the premise that magnetic substances (in this case ferromagnetic minerals) have a remnant magnetization, recording the magnetic fields that have acted on them. Rocks can acquire and retain such magnetizations in a number of ways, including thermal remnant magnetization (TRM), produced when a mineral cools below the Curie temperature in the presence of a magnetic field, and chemical remnant magnetization (CRM), a result of either the alteration or precipitation of a ferromagnetic mineral from solution, processes. Usually the most applicable to this type of study is detrital remnant magnetization (DRM), which is acquired during the deposition and lithification of sedimentary rocks (Butler, 1992). When ferromagnetic particles (usually titanomagnetite or hematite) encounter the sediment/water interface, they experience an aligning torque from the ambient magnetic field and, in laboratory models, rotate quite rapidly into alignment with the geomagnetic field present at the time of deposition (Butler, 1992).

However, in many cases particles can experience post-depositional realignment (pDRM) due to the fact that DRM is not mechanically locked until dewatering and consolidation of the sediments causes granular physical contact to inhibit motion (Butler, 1992). Realignment can occur as a result of processes like sediment compaction, in which inclination errors result from gravitational torque (known as “inclination shallowing”; Arason and Levi, 1990), viscous

remagnetization, or Brownian motion, a randomizing influence as the thermal energy of water molecules jostles smaller submicron to micron sized particles (Butler, 1992). Consequently, sedimentary deposits contain a combination of DRM and pDRM, though timescales for consolidation and grain-size attributes in fine-grained marine sediments are generally such that these differences are indiscernible within the bounds of polarity intervals. These facts and the observation that formations such as the Scaglia Cinerea are continuous rock records makes them useful for paleomagnetic reversal investigations, which involves tying geomagnetic field configurations to corresponding stratigraphic levels, and correlation to the geomagnetic polarity timescale (GPTS).

For the Monte Cagnero samples, nearly all possessed a low-stability overprinting close to the present local field (PLF) probably due to viscous remagnetization (VRM). This field was universally removed (i.e. unblocked) by either controlled-atmosphere thermal demagnetization to around 300°C (250°C to 340°C), or alternating frequency demagnetization to 15 mT, as depicted in the Zijderveld, J/Jo and equal area projections (Figs. 4, 5, 6). An unblocking temperature in this range is indicative of Fe-sulfides such as pyrrhotite (Wehland et al., 2005), which is a common alteration mineral in the pelagic sequences of Italy (Freeman, 1986). Some samples also contained a low-stability overprint that had unblocking temperatures between 100°C and 125°C, indicative of alteration and weathering to goethite (McElhinny and McFadden, 2000) , which is visible as brown staining in the effected cores and hand samples. The primary ChRM in all samples appears to be carried by a component with unblocking temperatures between 570°C and 580°C (some as low as 550°C), and coercivities around 40 mT, above which all thermal (TT) samples and some AF samples became directionally unstable (see Fig. 6), though many AF samples

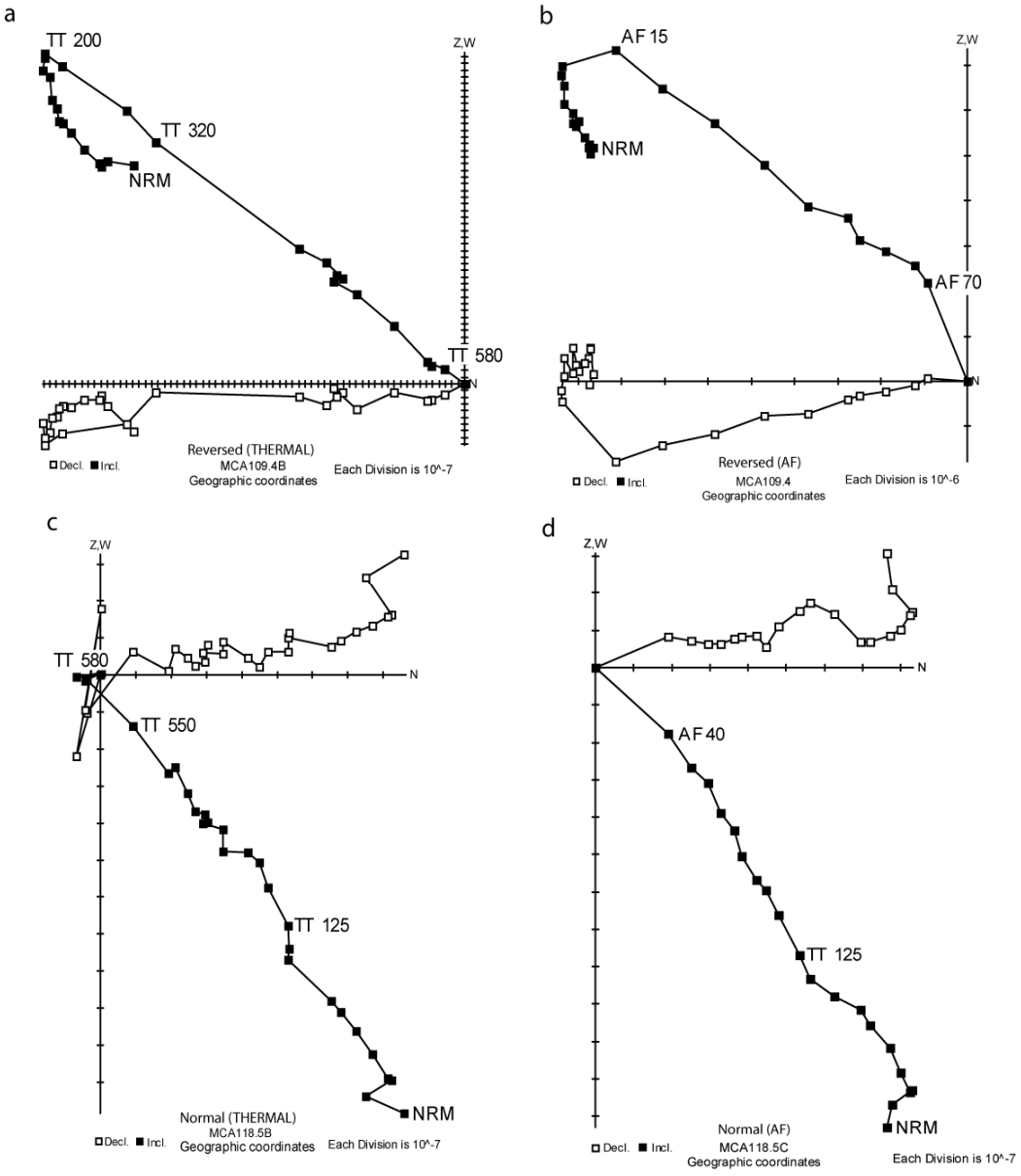

Figure 4. Zijderveld vector diagrams for selected representative Scaglia cinerea samples (A) thermal demagnetization of reversed sample 109.4B, (B) alternating frequency demagnetization of reversed sample 109.4, (C) thermal demagnetization of normal sample 118.5B, and (D) alternating frequency demagnetization of normal sample 118.5C. Numbers on graph indicate demagnetizing field in mT or heating temperature in °C. All projections are on vertical E-W planes.

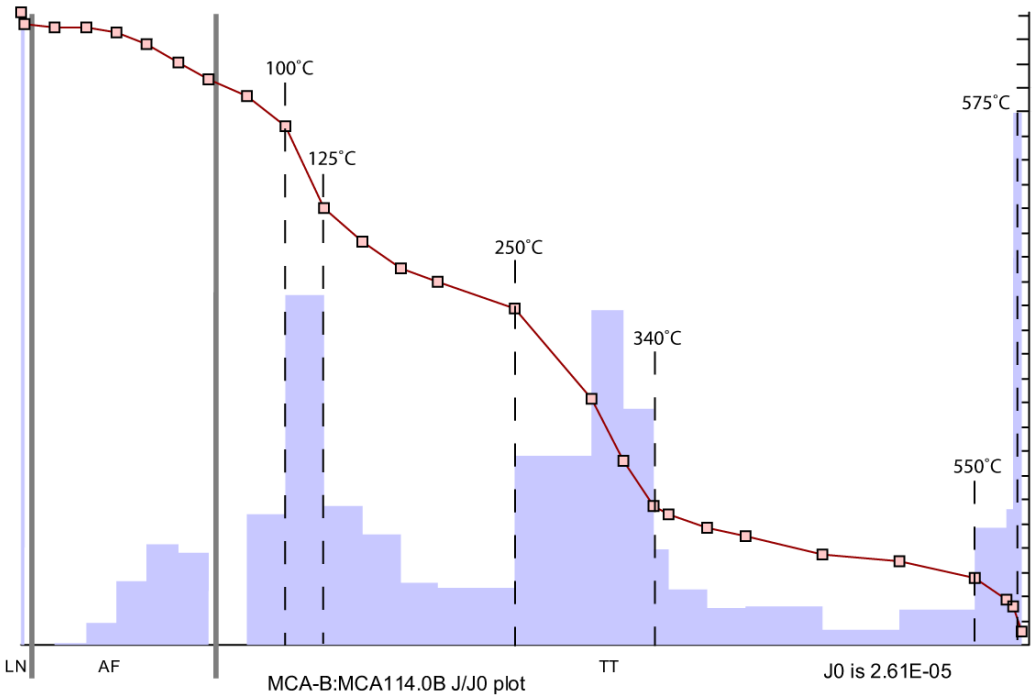

Figure 5. J/Jo plot for thermal sample 114.0B. Shaded bars indicate magnitude (%) change in magnetization, while points indicate total magnetization of the sample. Dotted lines with corresponding temperature markings delineate zones with a high rate of demagnetization, indicative of unblocking points for ferromagnetic minerals.

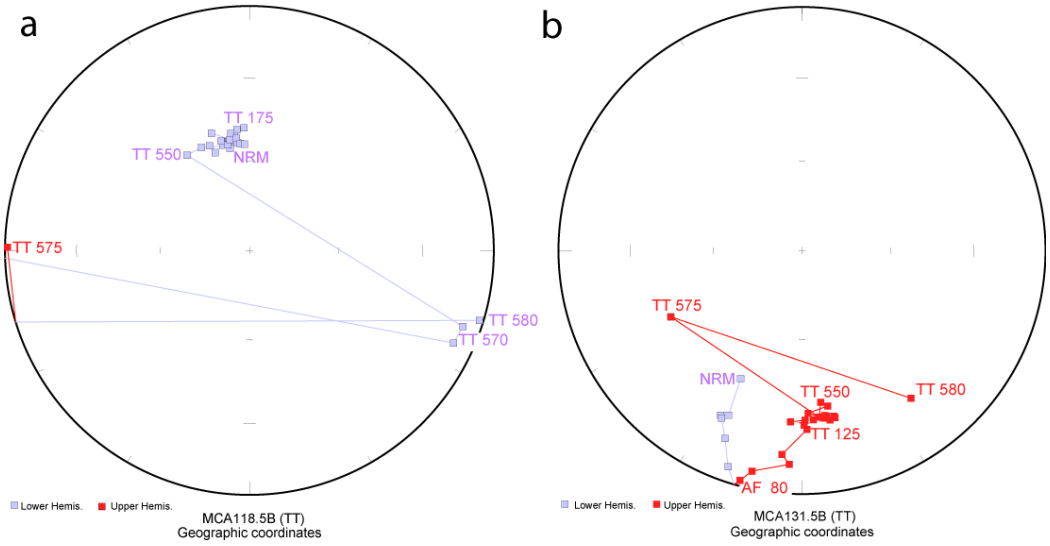

Figure 6. Equal-area stereograms of stepwise thermal demagnetization in (A) normal sample 118.5B and (B) reverse sample 131.5B. Numbers on plot indicate heating temperature in °C.

remained stable through the endpoint at 70 mT. This is indicative of a primary ChRM carrier of (titano)magnetite, with the possibility of the minimal presence of another higher-stability/coercivity carrier (such as hematite, unblocking temperature 675°C) in some samples (Freeman, 1986). For both thermal and AF groups, the high-stability component was interpreted as the ChRM vector, and least-squares models were forced through the origin as they decayed (Fig. 4), resulting in reverse and normal polarity stable components.

Progressive thermal and alternating frequency demagnetization steps defined stable ChRM endpoint groups (Fig. 7) of reverse and normal polarity at magnetic intensities of ~10% NRM ($<10^{-6}$ G). These endpoint clusters have a fairly small scatter for both polarity groups (Fig. 7), with few samples displaying declinations or inclinations that are intermediate between normal and reverse, meaning that the interpretation of the magnetozones is straightforward. A few samples experienced misorientation during the sampling and handling processes, but these samples were pre-identified and corrected during the analysis and plotting (all samples were corrected for bedding tilt during the sampling and orientation processes). The ChRM polarity clusters form two nearly antipodal groups (Fig. 7), and the confidence ellipses do not overlap, indicating that the mean directions are statistically different (Fisher, 1953). An F-ratio test reaffirms that they are statistically different at a 95% confidence level (all F-ratios were greater than the proposed null hypothesis; Watson, 1956, 1960). The vector mean directions for the polarity clusters (Appendix 1) from dataset A-C (AF demagnetization) are D= 343°, I= 51° (a_{95}= 5.9) and D= 169°, I= -54° (a_{95}= 5.0), while from dataset B (TT demagnetization) they are D= 343°, I= 53° (a_{95}= 7.6) and D= 164°, I= -40° (a_{95}= 4.0).

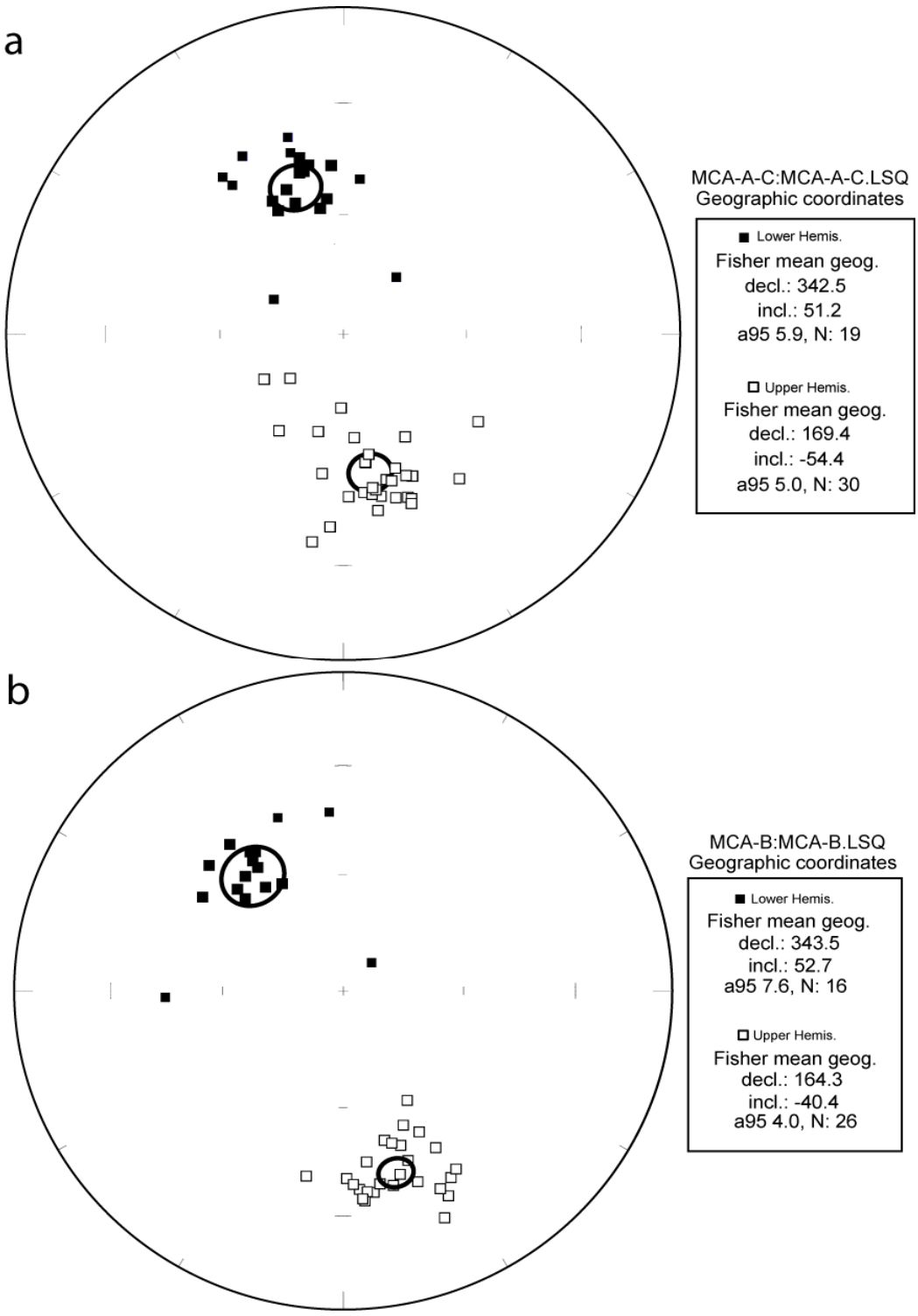

Figure 7. Equal-area stereograms of stable endpoint (ChRM) directions for (A) dataset MCA-A/C, alternating frequency demagnetization, and (B) dataset MCA-B, thermal demagnetization. Ellipses indicate Fisher confidence intervals for endpoint groups. All samples corrected for simple bedding tilt.

The two datasets show slight differences in both declination and inclination, some of which were found to be statistically significant, so for virtual geomagnetic pole (VGP) and associated calculations, thermally demagnetized dataset B (n=41) was used as the primary source due to anticipated inaccuracies resulting from unresolved high-coercivity components present in samples from the AF demagnetized samples from dataset A-C.

When plotted stratigraphically as a local magnetic polarity scale (Fig. 8), the vectors from individual samples within the polarity groups define four distinct magnetozones and at least two shorter reversal periods in the Monte Cagnero section. Each of the magnetozones is supported by numerous data points, and corroborated by both datasets in terms of position and duration, while the smaller polarity periods are supported by either one or two data points in each dataset (also coincident in space and time between sets). Resolution of magnetostratigraphy is poor between meters 126 and 145 due to lithologic complications (soft, wet marl), making their interpretation somewhat ambiguous, though data on either side is distinct and appropriate for good correlations.

A virtual geomagnetic pole (VGP) was calculated for each data point after the model of Kirschvink (1980). These points (Fig. 9) show a clear, consistent latitudinal ($\lambda°$) trend with an average pole position of 71° N (a_{95}= 2.4°). The longitudinal ($\phi°$) data is far more scattered and unclear, though there does appear to be a directed trend with an average position of 209° E (a_{95}= 32.0°).

Due to technical issues with coordinate system calibrations of the AMS system, we were unable to calculate stereographic poles (after Barton and McFadden, 1996) for the axes of anisotropy or quantify bulk susceptibility (*k*) for the samples throughout the stratigraphy, and therefore do not have data on the direction of

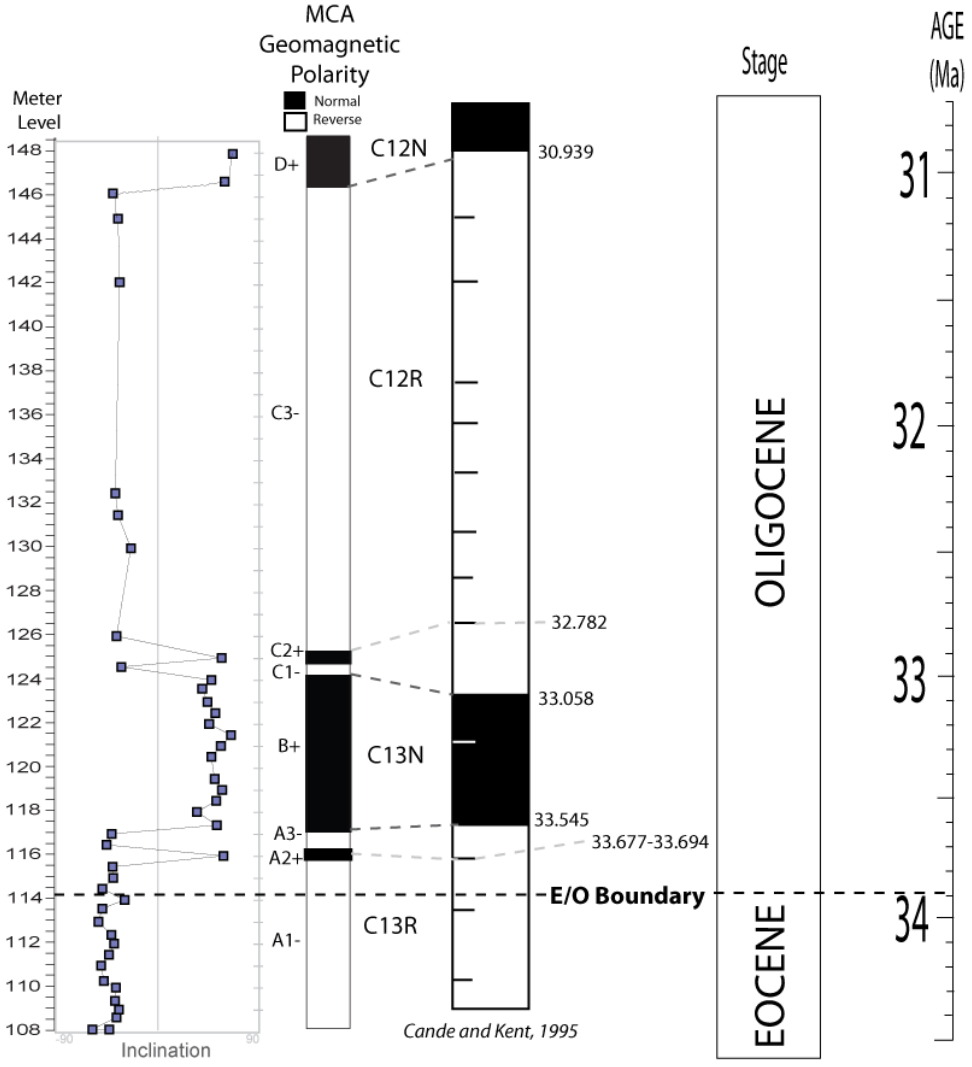

Figure 8. Stratigraphic variation of inclination, the interpreted polarity zones for the Monte Cagnero outcrop, and its correlation to the defined magnetozones of the geomagnetic polarity timescale (GPTS) of Cande and Kent (1992, 1995). In the timescale of Cande and Kent (1992, 1995), short bars indicate identified "cryptochrons", and numbers indicate interpolated ages (Ma).

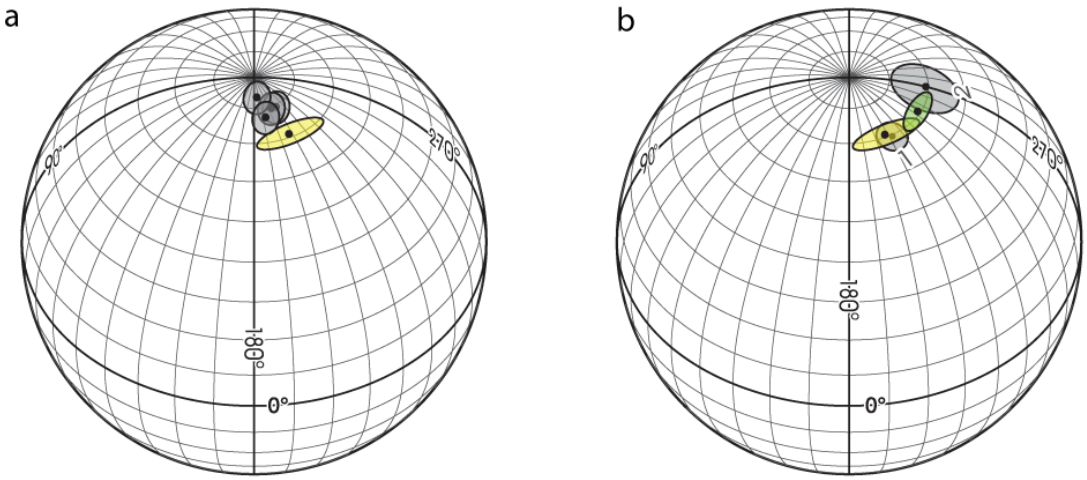

Figure 9. Spherical geographic projections of virtual geomagnetic poles (VGP). (A) VGPs plotted in gray with confidence intervals for 40 Ma- 25 Ma (Besse and Courtillot, 2002), and in yellow for Monte Cagnero data time-averaged from 34 Ma-31 Ma. (B) 1. VGP for African Plate from Eocene-Oligocene transition (Marton, 2006) and 2. VGP for Adrian microplate from Early Oligocene (Marton, 2006). VGP for Monte Cagnero replotted in yellow, corrected data (removal of Late-Eocene outliers) displayed in green.

LF-normed principle susceptibilities								LF-anisotropy factors				
Sample #	K_1	K_1 error	K_2	K_2 error	K_3	K_3 error	K_m	L	F	P	Tj	Pj
112.4	1.0076	0.0007	1.0068	0.0007	0.9855	0.0006	0.999967	1.001	1.022	1.022	0.92837	1.036228
114.5	1.0144	0.0002	1.0133	0.0002	0.9723	0.0002	1	1.001	1.042	1.043	0.948808	1.070745
118.5	1.0283	0.0106	0.9932	0.0105	0.9785	0.0106	1	1.035	1.015	1.051	-0.39924	1.074707
130	1.0234	0.0002	1.0187	0.0002	0.9579	0.0001	1	1.005	1.064	1.068	0.860812	1.110118
							Average	**1.0105**	**1.03575**	**1.046**	**0.584687**	**1.072949**
							Standard Deviation	**0.016442**	**0.022036**	**0.019096**	**0.657029**	**0.03021**

Table 1. Primary AMS data on principle susceptibilities and calculated (after Jelinek, 1978; Ferre et al., 2005) anisotropy factors.

preferential magnetization. The principle axes and basic information calculated on anisotropy are shown in Table 1, but further results will require reanalysis of at least one sample from each identified magnetozone and for each lithology.

Discussion

Four distinct magnetozones and two "cryptochrons" (e.g. Lanci et al. 1996) are identified at Monte Cagnero (Fig. 8) throughout the 40 meter section for a complete local magnetic polarity scale (LMPS) which is comparable to the official geomagnetic timescale as assembled by Cande and Kent (1992, 1995). When the LMPS is tied to known ages within the section, such as the E/O boundary (as defined by Parisi et al., 1988; Premoli Silva and Jenkins, 1993, and identified by Montanari et al., 2007; Tori and Monechi, 2007) and volcaniclastic layers (dated by Montanari et al., 1988), and extrapolated based on the assumption of constant deposition rates throughout the section, it matches the geomagnetic polarity timescale very closely (Fig. 8). Murphy (*unpublished)* reports sedimentation rates of 12.7 m/m.y. for the outcrop based on cyclostratigraphic analysis, while Tori and Monechi (2007) report a higher rate of 13.6 m/m.y.; however, for interpretations in this paper, a sedimentation rate of 15.2 m/m.y. was used. This rate was calculated based on independent time constraints within this section of the outcrop, specifically; the E/O boundary, dated via cyclostratigraphy at the Massignano GSSP by Jovane et al. (2006) and recognized at the Monte Cagnero outcrop by Tori and Monechi (2007), and a pair of biotite-rich volcaniclastic layers near the top of the outcrop which were $^{40}Ar/^{39}Ar$ dated by Montanari et al. (1988).

Stratigraphically, the first short reversal, or cryptochron, labeled A2+ in the LMPS (Fig. 8) occurs roughly 1.3 meters up-section of the E/O boundary (C13r.14),

which gives it a calibrated age of 33.615 Ma, slightly younger than the reported age of its interpreted correlation to identified cryptochron C13r-1 which lasts from 33.694 Ma to 33.677 Ma. The start of the longer normal polarity interval, referred to as zone B+ in the LMPS (Fig. 8), is interpreted as C13n because it is present at meter level 117.4, or 2.9 meters up-section of the boundary, providing a calibrated age of 33.509 Ma, less than 0.05 Ma younger than the start of C13n as reported by Cande and Kent (1995). Polarity zone C1- occurs approximately at meter 124.6, with an age of 33.033 Ma, and is interpreted as chron C12r, due to the fact that its reversal age is once again less than 0.05 Ma younger than that of Cande and Kent (1995). LMPS zone C2+ (Fig. 8) is then extrapolated to 32.873 Ma, equivalent to the geomagnetic timescale reported age of 32.782 for cryptochron C12r-8. The final reversal, zone D+, occurs at a stratigraphic level of 146.5m, and when calibrated to the biotite-rich volcaniclastics at meter 144.8 in Montanari et al. (1988; dated to 31.1 Ma), provides an extrapolated age of 30.972 Ma and allows for its interpretation as the beginning of C12n; only slightly different than the geomagnetic timescale reversal age of 30.939 Ma. Additionally, the duration of interpreted chron C13n is 0.476 m.y., while the GPTS reported length is 0.487 million years.

With the interpreted correlation to the GPTS, the outcrop at Monte Cagnero can effectively be linked to other major sections in Italy, such as the Contessa sections, the Massignano Quarry and the MassiCore. These sections are all of different lengths and possess magnetic data of varying resolution, but can be correlated to each other and the GPTS (Fig. 10). When scaled similarly and tied to the Eocene-Oligocene boundary (which has been identified at each outcrop to within 0.5m precision), the local magnetic polarity timescales and their interpreted chrons are extremely similar in both position (temporal, stratigraphic) and in duration (based

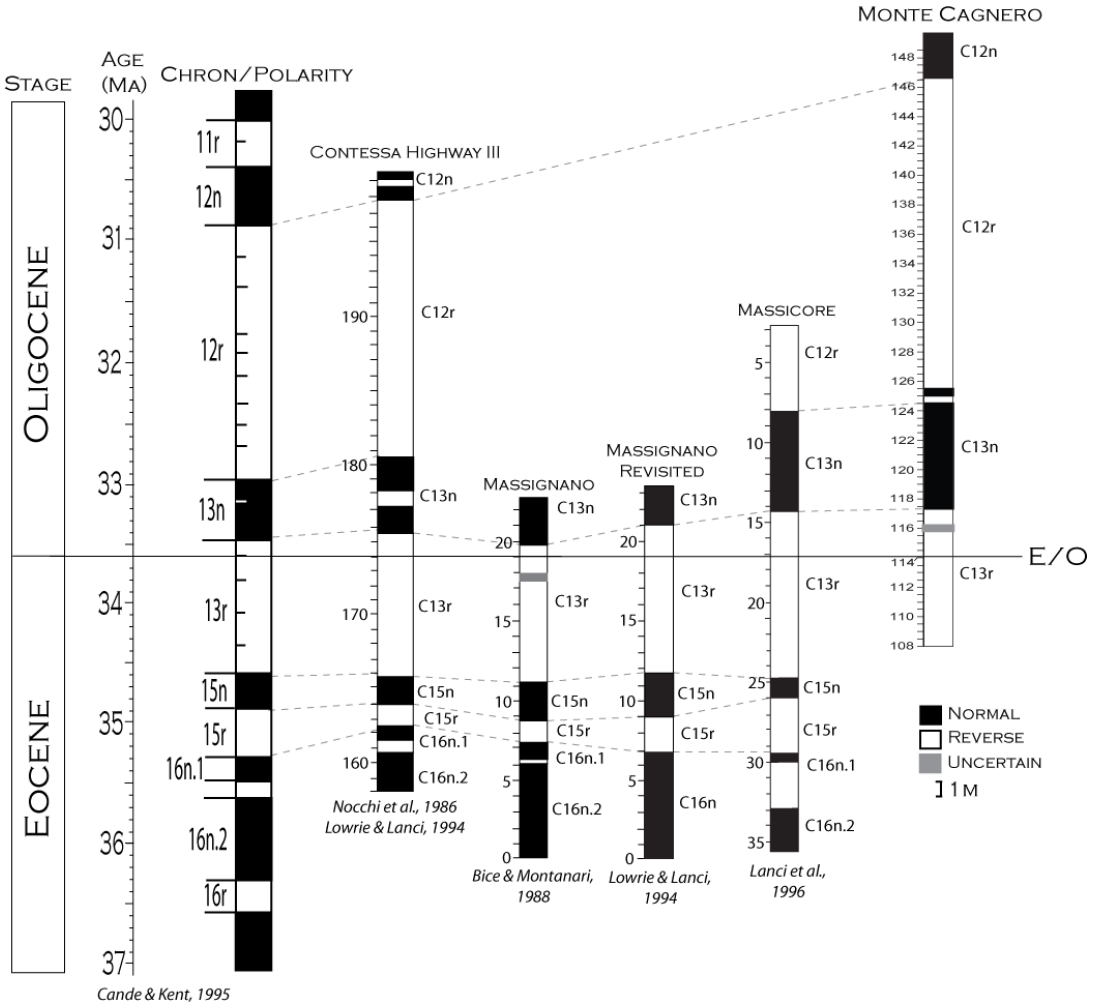

Figure 10. Comparison between geomagnetic polarity timescale (GPTS) of Cande and Kent (1992, 1995) and the magnetostratigraphies of the Monte Cagnero (this work), Contessa Highway (Nocchi et al., 1986; Lowrie and Lanci, 1994), Massignano (Bice and Montanari, 1988; Lowrie and Lanci, 1994) and MassiCore (Lanci et al., 1996) sections. Timescales are scaled and tied to the Eocene-Oligocene boundary, short bars indicate identified "cryptochrons" in the timescale.

on individual sedimentation rates constrained by alternate chronologies), therefore allowing for the unambiguous interpretation of Monte Cagnero as contemporaneous, continuous, and correlatable to the other pelagic sequences of the Northeastern Apennines.

The VGP data allows for the application of the Monte Cagnero magnetometry to paleogeography, and the plotting of a rough apparent polar wander (APW) pole for Italy across the Eocene-Oligocene transition. The calculated average VGP pole for this section (λ= 71°, ϕ=209°) for the time interval from roughly 34 Ma to 31 Ma fits the synthetic APW path for Adria/northern Africa during this period relatively well (Fig. 9); Besse and Courtillot (2002) and Muttoni (2001) report the African pole at λ= 78.9°, ϕ=201.7° for 35 Ma, and at λ= 79°, ϕ=207.7° for 30 Ma. However, many aspects of the Monte Cagnero magnetometry data make the correlation to Besse and Courtillot (2002) and Muttoni (2001) suspect. Primarily, field orientation techniques did not sufficiently locate the cores in three-dimensional space, making them less appropriate for the plotting of VGPs (though still high-quality magnetostratigraphy points). Regardless of this fact, other important geologic issues complicate the explanation of the VGP data, such as tectonic rotation and inclination shallowing.

The wide spread in the longitudinal data (a_{95}= 32.0°) could be a result of tectonic rotation of segments of the Adrian promontory (African Plate), specifically in the Umbria region which underwent a 20-25° counterclockwise rotation in the Paleocene and Eocene (Lanci et al., 1996; Marton, 2006). As Monte Cagnero is unambiguously part of the Umbria region and the Adrian microplate specified by both Lanci et al. (1996) and Marton (2006; despite a good fit to the African pole reported in that work), it could have experienced some of this tectonic rotation, skewing the longitudinal component. When outliers are removed from the dataset (interestingly,

all of the outliers occur within the first 10m of the outcrop, nearer/during the rotational events), the VGP longitude for the section across the Eocene-Oligocene transition becomes 241° (a_{95}= 15.5°), similar to the longitude of the rotated Adria pole of 270° for the Late Eocene reported by Marton (2006; Fig. 9).

The unfortunate lack of usable AMS poles makes conclusions on inclination shallowing purely speculative. However, calculated anisotropy factors (Table 1) show that the strain ellipses for the Scaglia Cinerea Formation are fairly round (Pj= 1.07 ± 0.03), indicating they have not undergone much tectonic or other major deformation, and are somewhat vertically oblate (Tj= 0.58 ± 0.66), suggesting that they could have been compressed/compacted unidirectionally (Arason and Levi, 1990; Ferre et al., 2005). While the direction of anisotropy and the orientation and magnitude of compression (indicated by strain ellipses) is unknown, these data are consistent with sediment compaction, which may be correlated to inclination shallowing. Additionally, the calculated VGP for the Monte Cagnero data is approximately 8° shallower than Besse and Courtillot's (2002) predicted value for the time period, again supporting that some inclination shallowing during compaction has taken place. Lanci et al. (1996) report average shallowing in inclinations for various Scaglia Cinerea Formation outcrops in the Umbria region (Contessa, Massignano) of between 5° and 10°, with as much as 15° shallowing in the MassiCore, which is consistent with the difference between this study's findings in the Monte Cagnero outcrop and the predictions of Besse and Courtillot (2002).

Conclusions

Paleomagnetic data for Monte Cagnero enables the assignment of a relative date for the age of the bottom of the section (fault/slump at roughly 34.129 Ma), and

more importantly provides an excellent correlation between this section and the GSSP at Massignano (chrons C13r through C12n, including some identified cryptochrons). Since these two locations have been definitively correlated via magnetostratigraphy, the sections can be linked together as a continuous record of the Eocene-Oligocene transition and associated environmental/ecological changes in central Italy (also providing a continuous section between the Eocene-Oligocene boundary and the Oi1 and other climatic events). The tentative fit to a synthetic apparent polar wander (APW) path serves to place the section and Adria as a whole on an otherwise poorly constrained paleogeographic map for the Eocene and Oligocene, especially with regard to the African Plate. This study further constrains the section and provides a record of the events of the Late Eocene and Oligocene, which could have major implications for understanding the processes and results of these global changes. Additionally, this work serves as basic chronostratigraphic groundwork for necessary in-depth future research on stable isotopes, mineralogy, and chemo- and biostratigraphy (or even further magnetostratigraphy) on the section to further support that the Monte Cagnero site is a viable option for consideration in the relocation of the global stratotype section and point (GSSP) for the Eocene-Oligocene boundary.

Acknowledgements

I would like to thank Sandro Montanari (OGC) for sparking my interest in paleomagnetism, encouraging me to undertake this project, and his tireless work in the field; Cam Davidson and Sarah Titus (Carleton College) for providing general guidance and comments and input on this paper; David Evans (Yale) for graciously allowing me to use the Yale Paleomagnetism Lab and taking time to help out in the lab, fixing my stupid mistakes, and answering lingering questions about the process; Ross Mitchell (Yale) for providing a great place to stay and work, a fallback for problems in the lab work, and information and tips on paleomagnetics; Aaron Fricke for help in the field and throughout the late nights of the insane drilling/orienting process; Spider Mariani (OGC), Paul Kopsick, Perry Spector, Lauren Colwell, Phil Varela, and Katie Marks for their help in the field and at OGC; Walter Alvarez (UC Berkeley) for not killing us in the night as we drilled cores right beneath him; the Carleton College Geology Department for funding the project; and geology majors of the past, present, and future for support (emotional and physical), food and shelter, and amusement throughout the research and writing process.

References

Alvarez, W., and Montanari, A., 1988, The Scaglia Limestones (Late Cretaceous-Oligocene) in the Northeastern Apennines Carbonate Sequence: Stratigraphic Context and Geological Significance: International Subcommittee on Paleogene Stratigraphy, Eocene/Oligocene ad hoc meeting, Ancona, IT, v. Special Publication 1, no. 1, p. 13-29.

Arason, P., and Levi, S., 1990, Models of Inclination Shallowing During Sediment Compaction: Journal of Geophysical Research, v. 95, no. B4, p. 4481-4499.

Barton, C., and McFadden, P., 1996, Inclination shallowing and preferred transitional VGP paths: Earth and Planetary Science Letters, v. 140, p. 147-157.

Besse, J., and Courtillot, V., 2002, Apparent and true polar wander and the geometry of the geomagnetic field over the last 200 Myr: Journal of Geophysical Research, v. 107, no. B11, p. 6/1-6/31.

Bice, D., Montanari, A., 1988, Magnetic stratigraphy of the Massignano section across the Eocene-Oligocene boundary: The Eocene-Oligocene boundary in the Marche-Umbria Basin (Italy); Interdisciplinary studies presented at the Eocene-Oligocene boundary ad hoc meeting, p. 111-117.

Bodiselitsch, B., Montanari, A., Koeberl, C., Coccioni, R., 2004, Delayed climate cooling in the Late Eocene caused by multiple impacts: high-resolution geochemical studies at Massignano, Italy: Earth and Planetary Science Letters, v. 223, p. 283-302.

Bohaty, S., Palike, H., Zachos, J., 2007, Deep-sea stable isotope and cycle stratigraphy of the Eocene-Oligocene transition: Global correlation of records and key problems in ongoing studies.: GSA Penrose Special Bulletin, p. 4.

Brown, R., *unpublished*, A Cyclostratigraphic Analysis of the Eocene-Oligocene Boundary GSSP, Massignano, Italy: Northfield, Carleton College, p. 58.

Butler, R., 1992, PALEOMAGNETISM: Magnetic Domains to Geologic Terranes, *in* Meader, N., ed., Blackwell Scientific Publishers.

Cande, S., and Kent, D., 1992, A new geomagnetic Polarity Time Scale for the late Cretaceous and Cenozoic: Journal of Geophysical Research, v. 97, p. 13,917-13,951.

-, 1995, Revised calibration of the geomagnetic polarity time scale for the late Cretaceous and Cenozoic: Journal of Geophysical Research, v. 100, p. 6093-6095.

Coccioni, R., Monaco, P., Monechi, S., Nocchi, M., Parisi, G., 1988, Biostratigraphy of the Eocene-Oligocene Boundary at Massignano (Ancona, IT): International Subcommittee on Paleogene Stratigraphy, Eocene/Oligocene ad hoc meeting, Ancona, IT, v. Special Publication 2, no. 1, p. 59-80.

Coccioni, R., Montanari, A., Bellanca, A., Bice, D., Brinkhuis, H., Church, N., Deino, A., Lirer, F., Macalady, A., Maiorano, P., Marsili, A., McDaniel, A., Monechi, S., Neri, R., Nini, C., Nocchi, M., Pross, J., Rochette, P., Sagnotti, L., Sprovieri, M., Tateo, F., Touchard, Y., Van Simaeys, S., Williams, G., *in press*, Integrated stratigraphy of the Oligocene pelagic sequence in the Umbria-Marche basin (Northeastern Apennines, Italy): A potential GSSP for the Rupelian/Chattian boundary.

Farley, K. A., Montanari, A, Shoemaker, Eugene M, Shoemaker, C S, 1998, Geochemical evidence for a comet shower in the late Eocene: Science, v. 280, no. 5367, p. 1250-1253.

Ferre, E., Tikoff, B., and Jackson, M., 2005, The magnetic anisotropy of mantle peridotites: Example from the Twin Sisters dunite, Washington: Tectonophysics, v. 398, p. 141-166.

Fisher, R., 1953, Dispersion on a Sphere: Proceedings of the Royal Society of London: Series A, Mathematical and Physical Sciences, v. 217, no. 1130, p. 295-305.

Freeman, R., 1986, Magnetic Mineralogy of Pelagic Limestones: Geophysical Journal International, v. 85, no. 2, p. 433-452.

Jelı´nek, V., 1978, Statistical processing of anisotropy of magnetic susceptibility measured on groups of specimen: Studia Geophyzika et Geodetika, v. 22, p. 50-62.

Jovane, L., Florindo, F., Sprovieri, M., Palike, H., 2006, Astronomic calibration of the late Eocene/early Oligocene Massignano section (central Italy), Geochemistry, Geophysics, Geosystems, p. 1-10.

Kirschvink, J., 1980, The least-squares line and plane and the analysis of palaeomagnetic data: The Geophysical Journal of the Royal Astronomical Society, v. 62, no. 3, p. 699-718.

Lanci, L., Lowrie, W., Montanari, A., 1996, Magnetostratigraphy of the Eocene/Oligocene boundary in a short drill-core: Earth and Planetary Science Letters, v. 143, p. 37-48.

Lanci, L., and Lowrie, W., 1997, Magnetostratigraphic evidence that ‘tiny wiggles’ in the oceanic magnetic anomaly record represent geomagnetic paleointensity variations: Earth and Planetary Science Letters, v. 148, p. 581-592.

Lowrie, W., Alvarez, W., Napoleone, G., Perch-Nielsen, K., Premoli Silva, I., and Toumarkine, M., 1982, Paleogene stratigraphy in Umbrian pelagic carbonate rocks: the Contessa Sections, Gubbio: Geological Society of America Bulletin, v. 93, p. 414-432.

Lowrie, W., and Lanci, L., 1994, Magnetostratigraphy of Eocene-Oligocene boundary sections in Italy; no evidence for short subchrons within chrons 12R and 13R: Earth and Planetary Science Letters, v. 126, no. 4, p. 247-258.

Marton, E., 2006, Paleomagnetic evidence for Tertiary counterclockwise rotation of Adria with respect to Africa, *in* Pinter, N., Grenerczy, G., Weber, J., Stein, S., Medak, D., ed., The Adria Microplate: GPS Geodesy, Tectonics and Hazards, Springer Earth and Environmental Sciences.

McElhinny, M., and McFadden, P., 2000, Paleomagnetism: Continents and Oceans, International Geophysics Series: San Diego, Academic Press, p. 386.

McFadden, P., and McElhinny, M., 1990, Classification of the reversal test in palaeomagnetism: Geophysical Journal International, v. 103, no. 3, p. 725-729.

Montanari, A., Deino, A., Drake, R., Turrin, B., DePaolo, D., Odin, G., Curtis, G., Alvarez, W., Bice, D., 1988, Radioisotopic dating of the Eocene/Oligocene boundary in the pelagic sequence of the northern Apennines: International Subcommission on Paleogene Stratigraphy, Special Publication, Aniballi, Ancona, p. 195-208.

Montanari, A., and Koeberl, C., 2000, Impact Stratigraphy- the Italian Record: Lecture Notes in Earth Sciences, v. 93, p. 364.

Montanari, A., Bice, D., Brinkhuis, H., Cleaveland, L., Coccioni, R., Farley, K., Monechi, S., Murphy, B., Tori, F., 2007, Integrated stratigraphy across the Eocene-Oligocene transition in the Monte Cagnero section (Northeastern Apennines, Italy): correlation with the GSSP of Massignano: GSA Penrose Special Bulletin, p. 57-58.

Murphy, B., *unpublished*, Cyclostratigraphic Analysis of pelagic carbonates and astronomical correlation in the Early Oligocene at Monte Cagnero (Piobbico, Italy): Northfield, Carleton College, p. 22.

Muttoni, G., Garzanti, E., Alfonsi, L., Cirilli, S., Germani, D., Lowrie, W., 2001, Motion of Africa and Adria since the Permian: paleomagntic and paleoclimatic constraints from Northern Libya: Earth and Planetary Science Letters, v. 192, p. 159-174.

Napoleone, G., 1988, Magnetostratigraphy in the Umbrian Pelagic Sequence: Review of the Development and its Finer Definition: International Subcommittee on Paleogene Stratigraphy, Eocene/Oligocene ad hoc meeting, Ancona, IT, v. Special Publication 1, no. 2, p. 31-56.

Nocchi, M., Parisi, G., Monaco, P., Monechi, S., Madile, M., Napoleone, G., Ripepe, M., Orlando, M. , 1986, The Eocene-Oligocene Boundary in the Umbrian pelagic sequence, Italy, *in* Pomerol, C., Premoli-Silva, I., ed., Terminal Eocene Events: Amsterdam, Elsevier, p. 15.

Odin, G., Clauser, S., Renard, M. , 1988a, Sedimentological and Geochemical Data on the Eocene-Oligocene Boundary at Massignano (Ancona, IT): International Subcommittee on Paleogene Stratigraphy, Eocene/Oligocene ad hoc meeting, Ancona, IT, v. Special Publication 3, no. 1, p. 175-188.

Odin, G. and Montanari, A., 1988b, The Eocene-Oligocene boundary at Massignano (Ancona, Italy): a potential boundary stratotype: International Subcommission on Paleogene Stratigraphy, Special Publication, Aniballi, Ancona, p. 253-263.

Parisi, G., Guerrera, F., Madile, M., Magnoni, G., Monaco, P., Monechi, S., Nocchi, M., 1988, Middle Eocene to early Oligocene calcareous nannofossil and foraminiferal biostratigraphy in the Monte Cagnero section, Piobbico (IT), *in* Premoli Silva, I., Coccioni, R., and Montanari, A., ed., The Eocene-Oligocene boundary in the Marche-Umbria Basin (Italy): International Subcommission on Paleogene Stratigraphy, Special Publication, Aniballi, Ancona, p. 119-135.

Premoli Silva, I., and Jenkins, D., 1993, Decision on the Eocene-Oligocene boundary stratotype: Episodes, v. 16, p. 379-382.

Prothero, D. R., 1994, The Eocene-Oligocene Transition: Paradise Lost: New York, Columbia University Press, 291 p.

Salamy, K., and Zachos, J., 1999, Latest Eocene–Early Oligocene climate change and Southern Ocean fertility: inferences from sediment accumulation and stable isotope data: Palaeogeography, Palaeoclimatology, Palaeoecology, v. 145, p. 61-77.

Tori, F., and Monechi, S., 2007, Paleoecological and paleoclimatical significance of calcareous nannofossils at the E/O transition: new data from the Cagnero and Massignano sections, Umbria-Marche area (Italy): GSA Penrose Special Bulletin, p. 77.

van Mourik, C., and Brinkhuis, H., 2005, The Massignano Eocene-Oligocene golden spike section revisited: Stratigraphy, v. 2, no. 1, p. 13-30.

van Mourik, C., Lourens, L., Brinkhuis, H., Pälike, H., Hilgen, F., Montanari, A., and Coccioni, R., 2007, From greenhouse to icehouse at the Massignano Eocene-Oligocene GSSP: implications for the cause, timing and effects of the Oi-1 glaciation: GSA Penrose Special Bulletin, p. 2.

Watson, G., 1956, Analysis of Dispersion on a Sphere: Monthly Notices of the Royal Society for Astronomy and Geophysics Supplement, v. 7, p. 153-159.

-, 1960, More Significance Tests on the Sphere: Biometrika, v. 47, no. 1-2, p. 87-91.

Wehland, F., Eibl, O., Kotthoff, S., Alt-Epping, U., Appel, E., 2005, Pyrrhotite pTRM acquisition in metamorphic limestones in the light of microscopic observations: Physics of the Earth and Planetary Interiors, v. 151, p. 107-114.

Zachos, J., Pagani, M., Sloan, L., Thomas, E., Billups, K., 2001, Trends, Rhythms, and Abberations in Global Climate 65 Ma to the Present: Science, v. 292, no. 5517, p. 686-693.

Zijderveld, J. D. A., 1967, A. C. demagnetization of rocks: analyses of results. , *in* Collinson, D. W., Creer, K. M. , Runcorn, S. K., ed., Methods in Paleomagnetism: New York, Elsevier.

Sample #	D (°)	I (°)	Error
108.65	174.1	-64	3.6
109	162.7	-46.5	3.5
109.4	169.2	-44.3	2.9
110	172.8	-49.6	3.8
110.3	167.3	-47.9	4.6
111	170.4	-57.2	3.1
111.5	142.1	-43.3	2.8
112	170.6	-57.4	3.4
112.4	194	-64.9	3.8
112.4C	181.7	-71.6	4.6
113	168.4	-59.2	3.9
113.6	170.1	-48.8	3.8
114	164	-51.8	9.2
114.0C	229.3	-73.1	4.5
114.5	154.7	-50.3	3.5
115	168.5	-49.8	2.5
115.5	149.7	-60.2	4.5
116	239.6	-67.8	5.3
116.0C	188.3	-36	8.9
116.5	178.2	-48.8	2.5
117	212.9	-61.2	4.6
117.4	344.2	41.9	1.4
118	346.4	43.8	3.6
118.1	345.2	47.7	5.2
118.5	356	47.1	4
118.5C	346.7	47.6	3.6
119	339.1	50.9	3.7
119.5	331.2	37.9	5.3
119.5C	332.7	52.2	3.7
120.5	348.7	46.2	2.8
121	323.3	39.9	5.6
121.5	297.3	71.1	5.1
122	344.7	37.6	4.7
122.5	42	70.9	1.8
122.5C	353.2	55.7	5.1
123	332.8	55.1	4.1
123.6	5.9	50.6	2.9
124	340.4	55	5.2
124.0C	324.1	43.2	2.9
124.6	183.8	-40.6	5.8
125	349.9	57.9	2.7
125.0C	---	---	---
125.5	188.4	-54.5	6.4
126	156.7	-51.1	6.3
130	159	-45.6	5.4
131.5	162.3	-51.1	4.5
132.5	169.5	-50.5	2.9
132.5C	159.4	-53.9	5.3
142.1	158.1	-44.9	5.8
142.1C	158.7	-43.7	5.2
145	123.8	-50.2	6.9

Sample #	D (°)	I (°)	Error
108.1	159.7	-42.7	1.8
108.1B	150.5	-57.6	2.4
108.65B	171.6	-36.3	2.4
109B	174.3	-34.2	2.2
109.4B	175.5	-37.6	2.1
110B	173.4	-36.7	2.5
110.3B	160.2	-47.3	1.6
111B	165.1	-49.9	2.7
111.5B	150.3	-42.8	2
112B	169.6	-38.4	2.1
112.4B	179	-40.8	2.2
113B	156.6	-52.1	2.2
113.6B	162.9	-48.6	2.3
114B	153.6	-29	2.6
114.5B	152.5	-48.7	1.2
115B	177.1	-39.1	2.7
115.5B	163.3	-39.7	8.7
116B	276.8	58.4	5.1
116.5B	172.5	-45	0.9
117B	191	-40.5	5.2
117.4B	345.6	52.5	2.6
118B	6.1	34.9	4.1
118.5B	351.1	52	3.3
119B	335.5	57.1	2.4
119.5B	321.4	50.5	5.1
120.5B	345.3	47.6	1.7
121B	336.8	56	1.2
121.5B	52.5	65	5.5
122B	342.9	45.6	3.2
122.5B	339.4	51	5.1
123B	337.2	44.2	3.1
123.6B	352.8	39.5	2.2
124B	343.2	47.5	3.6
124.6B	154.6	-31.9	6.7
125B	347.6	56.8	3.6
126B	159.3	-36.2	5.5
130B	156.6	-23.5	2.9
131.5B	174.8	-34.8	3.7
132.5B	166	-37.2	3
142.1B	150.8	-33.4	2.8
145B	148.5	-34.8	3

Dataset MCA-A/C (AF)

	D (°)	I (°)	Error	n
Normal	**342.5**	**51.2**	**5.9**	**19**
Reverse	**169.4**	**-54.4**	**5**	**31**

Dataset MCA-B (TT)

	D (°)	I (°)	Error	n
Normal	**343.5**	**52.8**	**7.9**	**15**
Reverse	**164.3**	**-40.4**	**4**	**26**

Appendix 1. ChRM vectors for Monte Cagnero samples.